Electrochimica Acta 56 (2011) 1409–1416

Contents lists available at ScienceDirect

Electrochimica Acta

journal homepage: www.elsevier.com/locate/electacta

On the gas-evolution efficiency of electrodes I – Theoretical

H. Vogt

Beuth University of Technology, Berlin, Germany

ARTICLE INFO

Article history:
Received 14 July 2010
Received in revised form 24 August 2010
Accepted 24 August 2010
Available online 17 September 2010

Keywords:
Gas-evolution efficiency
Gas-evolving electrodes
Bubble coverage
Mass transfer

ABSTRACT

At gas-evolving electrodes, the product of an electrochemical reaction, e.g. H_2 or O_2, does initially not exist as a gas but in dissolved form in the electrolyte liquid. Its appearance in the form of gas bubbles results from subsequent desorption. However, the process of desorption from the liquid phase into the gaseous phase is commonly not complete in the vicinity of the electrode or at all in the interelectrode space. The fraction of the product transferred into the gaseous phase of gas bubbles adhering to the electrode surface is termed the *gas-evolution efficiency*. This quantity is one of the controlling parameters in estimating the rate of microconvective mass transfer, the industrially most important mechanism. A theoretical investigation shows the impact of the bubble coverage – previously only derived from an analysis of experimental data in combination with an unsubstantiated perception – and gives information on further controlling quantities: the mass transfer coefficients of two competing mechanisms.

1. Introduction

Mass transfer at gas-evolving electrodes is controlled by various mechanisms acting simultaneously. Frequently one of the mechanisms is predominant. At small values of the current density the dominating mechanism is single-phase free convection due to density gradients within the liquid [1,2] in combined action with 2-phase free convection induced by rising bubbles [3,4]. Microconvective mass transfer is the controlling mechanism at mean and large current density values and might be the most important mechanism in application to industrial electrochemical reactors. Strong superimposed forced flow interferes with all of the above mechanisms [5,6].

The rate of gas evolution at electrodes is an important parameter in mass transfer, because bubbles growing at an electrode surface and finally breaking off induce near the electrode a microflow stirring the concentration boundary layer. In particular, the number of the simultaneously adhering bubbles, their growth velocity and their departure size are important parameters. All these quantities control the fraction of the electrode surface shaded by adhering gas bubbles. This parameter is commonly termed the bubble coverage Θ. It is well-known that the bubble coverage is controlled to a certain extent by the surface state of the electrode affecting the wettability [7] which is strongly affected by the electrode potential. So the bubble coverage and the rate of gas evolution are closely interrelated [8].

It may seem to make sense to quantitatively interrelate the rate of gas evolution and the bubble coverage with the current density simply by applying Faraday's law and the equation of state of an ideal gas. But there are some difficulties. When such attempts are made, a distinct discrepancy between estimate and experimental result is commonly found [9]. In fact, the rate of gas evolution at the electrode is smaller than the value calculated. The reason is that only a fraction of the total amount of substance produced at the electrode and entering the electrolyte liquid in the form of dissolved gas is transferred into the gaseous phase of bubbles adhering to the electrode surface.

The electrode product, e.g. hydrogen, may undergo chemical reactions with the electrode or at its surface or may be trapped in the electrode material or diffuse to the electrode rear side. Only the remaining enters the liquid and appears in dissolved form where it may subsequently undergo homogeneous or heterogeneous chemical reactions, Fig. 1. But even if such processes do not happen or are negligibly small, the rate of transfer of dissolved gas from the liquid into bubbles adhering to the electrode surface comprises only a fraction of the total rate. The complementary amount leaves the electrode boundary layer in dissolved form and is partly desorbed by freely moving bubbles and partly released from the interelectrode space still in dissolved form.

The fraction desorbed to adhering bubbles is an important operation parameter and has been termed the *gas-evolution efficiency* f_G. Out of the total amount of product generated at the electrode it denotes the fraction that is transferred by desorption from the liquid phase into the gaseous phase of adhering bubbles. This process is the one inducing bubble growth of adhering bubbles, and

E-mail address: Sci@helmut-vogt.de

0013-4686/$ – see front matter © 2010 Elsevier Ltd. All rights reserved.
doi:10.1016/j.electacta.2010.08.101

Nomenclature

A	electrode area [m^2]
A_a	active area of electrode [m^2]
A_δ	electrode area occupied by bubble boundary layer [m^2]
c	local concentration of dissolved gas [$mol\,m^{-3}$]
c_b	concentration at bubble surface [$mol\,m^{-3}$]
c_e	concentration at electrode surface [$mol\,m^{-3}$]
c_s	saturation concentration [$mol\,m^{-3}$]
c_∞	concentration in liquid bulk [$mol\,m^{-3}$]
d	equivalent break-off diameter [m]
$\bar{d}$	average diameter of adjacent bubbles [m]
D	diffusion coefficient [$m^2\,s^{-1}$]
f_G	gas-evolution efficiency
F	Faraday constant, $F = 96\,487\,A\,s\,mol^{-1}$
I	current [A]
n	number of simultaneously adhering bubbles
$\dot{N}$	molar rate of substance desorbed from electrode [$mol\,s^{-1}$]
p	liquid pressure in contact with gas bubble [$kg\,m^{-1}\,s^{-2}$]
r	coordinate parallel to electrode surface [m]
R	universal gas constant, $R = 8.3143\,kg\,m^2\,s^{-2}\,mol^{-1}\,K^{-1}$
T	temperature [K]
y	coordinate orthogonal to electrode surface [m]

Greek

γ	surface tension [$kg\,s^{-2}$]
δ_1	diffusion layer thickness of electrode [m]
δ_2	Nernst diffusion layer thickness of adhering bubbles [m]
Θ	fractional bubble coverage
ν_B	stoichiometric number of product
ν_e	charge number
ρ_G	gas density [$kg\,m^{-3}$]
ρ_L	liquid density [$kg\,m^{-3}$]
Φ	current efficiency

Dimensionless groups

Ja	Jakob number, Eq. (38)
Pe	Péclet number of mass transfer, Eq. (44)
Sh_1	Sherwood number of transfer to liquid bulk, Eq. (16)
Sh_2	Sherwood number of transfer to adhering bubbles, Eq. (10)

it is the growth velocity that affects microconvective mass transfer to or from the electrode. The complementary fraction does not contribute to that mechanism.

Estimating values of the mass transfer coefficient from available mass transfer equations requires the knowledge of values of the bubble coverage Θ as well as that of the gas-evolution efficiency f_G. The interrelation between the bubble coverage and the current density is known with fair accuracy [10]. A satisfactory interrelation of the gas-evolution efficiency with either the current density or the bubble coverage is not available so far. Only unsatisfactory approaches were made [11,12]. It is further not known what further parameters are active on the gas-evolution efficiency. In the following an attempt on the basis of a mathematical model is made to answer these open questions.

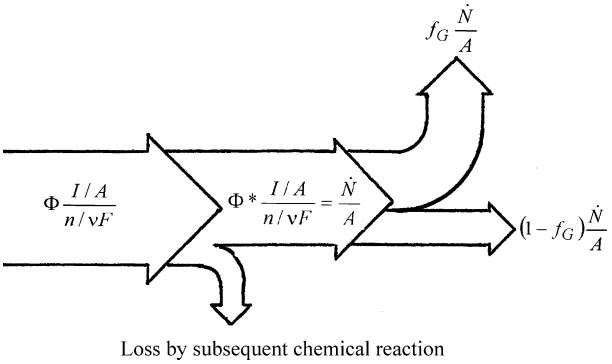

Fig. 1. Schematic split of the paths of dissolved gas in the electrode boundary layer.

2. Cognition of the gas-evolution efficiency

Baars and Kayser [13] stated that at small values of the current density only a fraction of the total hydrogen (or any other substance stable in gaseous phase under environmental conditions) generated by the electrochemical reaction (as estimated from Faraday's law) enters the gaseous phase of bubbles. The complementary fraction remains dissolved in the liquid and leaves the electrode space in dissolved form. Eucken [14] found that very high rates of the current density are necessary causing to disappear the discrepancy between the total rate of generated substance and the rate of substance transferred into the gaseous phase. In contrast, Roušar and Cezner [15] concluded from evaluation of bubble growth data that current densities above $10\,A\,m^{-2}$ are sufficient to consider the fraction remaining in solution negligible. Kadija et al. [16–18] observed that the transferred fraction was the smaller the larger the solution flow velocity past the electrode was. It has further been recognized that two completely different processes are active, namely a purely electrochemical process generating a substance existing in dissolved form after desorption from the electrode surface, and a purely physical process forming a gaseous phase consisting of bubbles adhering to the electrode surface, and both processes are not simply interrelated quantitatively [19]. The gas-evolution efficiency denoting the fraction of the transferred rate was introduced [20], and subsequently numerous efforts were made to describe it quantitatively on the basis of theoretical and experimental investigations [11,12,21–31]. Efforts to estimate the value of the gas-evolution efficiency depending on the controlling parameters continue.

3. Gas-evolution efficiency and bubble coverage

It is on hand that the rate of desorption is interrelated with the bubble coverage Θ. At very small values of the current density with nearly no bubbles adhering to the electrode, $\Theta \to 0$, i.e. with only a small area of the gas–liquid interface, the gas-evolution efficiency must be very small, $f_G \to 0$. On the other hand, when the electrode surface is overcrowded by adhering bubbles, $\Theta \to 1$, the gas-evolution efficiency is expected to approach the maximum value, $f_G \to 1$. In this case, nearly the total of dissolved gas is transferred into the gaseous phase [11].

The amount of dissolved gas passing from the liquid to the gas–liquid interface of adhering bubbles increases with increasing distance from the electrode surface. The maximum value is attained at the vertex of the adhering bubble. In case the bubble height is smaller than the concentration boundary layer of the electrode, the liquid remains supersaturated at that point. Further desorption of the dissolved gas may continue by freely moving bubbles within the boundary layer, but there is no impact on the growth of adhering bubbles. On the other hand, if the bubble height is larger than

the boundary layer thickness, any further desorption is meaningless since the supersaturation is small outside the boundary layer. Therefore, it is reasonable to restrict the gas-evolution efficiency to bubbles adhering to the electrode in agreement with a previous definition [11,32].

4. Mathematical model

It is too clear that every model involves a deformation of reality. In the following a mathematical model will be used sufficiently accurate to provide reliable information but sufficiently simple for a reasonable treatment of the problem. Several versions will be referred to for comparison.

The substance produced at the electrode enters the liquid and is transported from the active electrode area in direction to the liquid bulk. The transport mechanism of reactant in direction to the electrode is sufficiently complex due to the presence of adhering and freely moving bubbles. However, the transport of the dissolved gas from the electrode is substantially more complex, because there are two competing mass transfer mechanisms interfering with each other. One of the transports is that to the bulk, the other one is that to the bubbles adhering to the electrode surface. The superposition of both mechanisms complicates the concentration distribution within the electrode boundary layer.

4.1. Mass transfer to liquid bulk

A problem relates to the cross-sectional area available for transfer of dissolved gas from the electrode surface to liquid bulk. The area varies with the distance from the electrode since the shape of adhering bubbles is that of a segmented sphere or approximately a sphere. For the sake of simplicity, the area in each cross-section will be equated with an area

$$A_a = A(1 - \Theta) \tag{1}$$

defined by the total electrode area diminished by the partial area shaded by orthogonal projection of the bubble contour to the electrode surface [8,10]. This simplification is admissible since calculations have shown that the electrode area of the ring-shaped zone surrounding the bubble foot carries a negligibly small current density [33–35]. Θ denotes the fractional bubble coverage

$$\Theta \equiv n\frac{\pi}{4}\frac{\bar{d}^2}{A} \tag{2}$$

where n denotes the number of bubbles simultaneously adhering to the total electrode surface A, and $\bar{d}$ denotes a local and temporal average diameter during the residence time of bubbles at the electrode. The direction of transport of dissolved gas to the bulk is assumed to be orthogonal to the electrode surface.

$$\frac{dc}{dy} < 0 \tag{3}$$

4.2. Mass transfer to adhering bubbles

The superimposed competing mass transfer, the desorption into adhering gas bubbles, causes a complex concentration field of dissolved gas in liquid [12]. In contact with an adhering bubble, the concentration is small and depends on the curvature of the bubble interface. That means it varies during bubble growth. However, using an invariable average diameter $\bar{d}$ bypasses that problem. The gas–liquid interfacial concentration is thus [36]

$$\frac{c_b}{c_s} = 1 + \frac{4\gamma}{p\bar{d}}\frac{\rho_L}{\rho_L - \rho_G} \tag{4}$$

As the bubbles in aqueous solutions are very small, the concentration is not much larger than the saturation, $c_b/c_s \approx 1$.

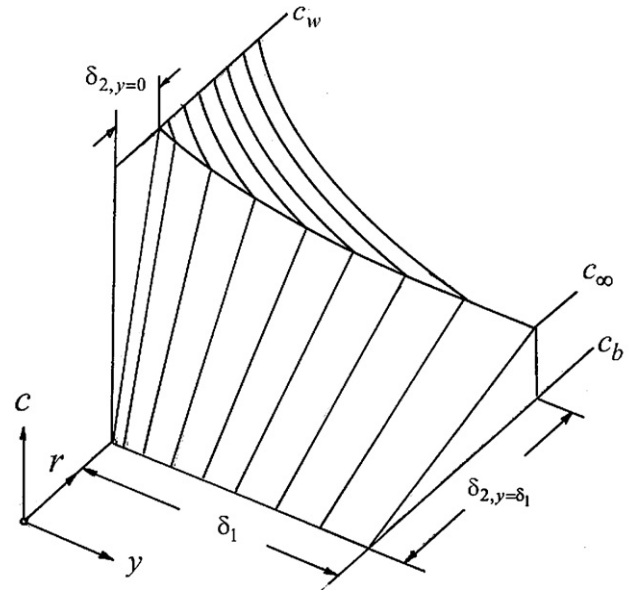

Fig. 2. Geometry of the model. Coordinates start from the centre of the circular contact area. Competing transport paths of dissolved hydrogen in y direction and in r direction.

With increasing distance from the bubble surface, the concentration increases until it reaches a maximum from where it decreases in direction to the neighbouring bubble. In the present treatment, the real concentration profile is substituted by that of a Nernst diffusion layer of thickness δ_2 in direction parallel to the electrode surface (although the real profile is not linear due to the curvature of the bubble surface). The rate of mass transfer of the desorption process is

$$d\dot{N}_2 = \frac{D}{\delta_2}dA_2(c - c_b) \tag{5}$$

and proceeds in direction to the bubble surface parallel to the electrode surface due to a concentration gradient

$$\frac{dc}{dr} < 0 \tag{6}$$

where the zero-point coincides with the centre of the contact area of the adhering bubble, Fig. 2. Outside the diffusion layer the concentration is supposed to be uniform in direction parallel to the electrode surface.

$$\frac{dc}{dr} = 0 \tag{7}$$

The differential bubble surface area of adhering bubbles is the projection area in direction parallel to the electrode surface,

$$dA_2 = n\pi\bar{d}\,dy = 4A\Theta\frac{dy}{\bar{d}} \tag{8}$$

resulting in

$$d\dot{N}_2 = 4\Theta Sh_2\frac{D}{d}A(c - c_b)\frac{dy}{\bar{d}} \tag{9}$$

where by definition

$$Sh_2 \equiv \frac{d}{\delta_2} \tag{10}$$

denotes the Sherwood number of this second transfer process, and $c = c(y) \neq c(r)$ is the concentration of dissolved gas outside the bubble boundary layer. The break-off diameter d of a sphere with equal volume is related to the average diameter $\bar{d}$

$$\bar{d} = \tfrac{2}{3}d \tag{11}$$

since the Fourier number during bubble growth is approximately constant [37,38].

4.3. Gas-evolution efficiency

By definition, the gas-evolution efficiency denotes the ratio of the rate $\dot{N}_2$ of dissolved gas transferred from a certain electrode area A by desorption from the liquid phase into the gaseous phase formed of bubbles adhering to the electrode surface divided by the total rate $\dot{N}$ of dissolved substance produced at the electrode area and entering the electrolyte liquid.

$$f_G \equiv \frac{\int_0^Y d\dot{N}_2}{\dot{N}} \tag{12}$$

The upper integration limit Y is variable. In case the adhering bubble does not penetrate the electrode boundary layer thickness, integration extends up to the bubble height. Since in electrolysis of aqueous solutions the contact angle is commonly very small [10], the total height of the bubble may be equated with the mean bubble diameter $\bar{d} = Y$. If the bubble height exceeds the boundary layer thickness, the upper integration limit is $Y = \delta_1$ (provided the liquid bulk is not considered supersaturated).

The local value of the gas-evolution efficiency

$$f = \frac{\int_0^y d\dot{N}_2}{\dot{N}} \tag{13}$$

increases steadily with increasing distance y from the electrode surface. Its value is $f = 0$ at the solid–liquid interface, $y = 0$, and reaches its final value $f = f_G$ at the vertex of the adhering bubble. The process of desorption may continue at larger values of y, because bubbles are present outside the bubble curtain near the electrode surface [39] and the liquid may be slightly supersaturated, but any such further desorption is unimportant.

The denominator in Eq. (12) can easily be taken from Faraday's law,

$$\frac{\dot{N}}{A} = \Phi^* \frac{I/A}{\nu_e/\nu_B F} \tag{14}$$

where $\Phi^* \leq \Phi$ denotes a factor equal to or smaller than the current efficiency since it comprises any possible losses of the product through subsequent homogeneous or heterogeneous reactions. I/A is the nominal current density on the total area regardless of the shaded fraction Θ. With the definition equation of mass transfer,

$$\frac{\dot{N}}{A} = \frac{D}{\delta_1}(c_e - c_\infty)_{f_G=0} \tag{15}$$

and by introducing a Sherwood number of mass transfer to the bulk,

$$Sh_1 \equiv \frac{d}{\delta_1} \tag{16}$$

follows

$$\frac{\dot{N}}{A} = Sh_1 \frac{D}{d}(c_e - c_\infty)_{f_G=0} \tag{17}$$

Sh_1 is known from available equations applicable to mass transfer in absence of a second superimposed process of desorption, such as for reactants. Therefore, the concentration difference is restricted to the condition $f_G = 0$.

4.4. Concentration profile in y direction

If the desorption was zero, the total rate of dissolved gas would be transferred from the electrode surface to the liquid bulk. The rate would not vary within the boundary layer of thickness δ_1. With Nernst's simplifying assumption that mass transfer proceeds solely by diffusion, the real concentration profile can be substituted by a linear one without remarkable inaccuracy. Convection in the layer is ignored. The concentration gradient is constant.

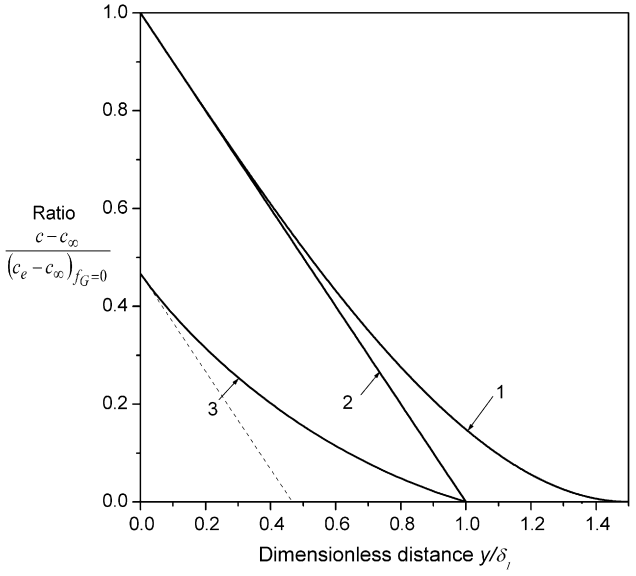

Fig. 3. (1) Real concentration profile without desorption or homogeneous reaction: diffusion + convection. (2) Idealized profile without desorption: diffusion, no convection (Nernst profile). (3) Idealized profile for gas-evolving electrodes: diffusion + desorption, no convection.

$$\frac{dc}{dy} = -\frac{c_e - c_\infty}{\delta_1} \tag{18}$$

However, the precondition of the Nernst profile is constant flux within the diffusion layer attached to the electrode surface. In case of desorption or homogeneous reaction within the boundary layer, the concentration profile will no longer be linear but curved without leaving the assumption of no convection, Fig. 3. Therefore, the concentration gradient varying with y must meet the following conditions.

- Immediately at the electrode surface, $y = 0$, where the liquid does not undergo desorption, the concentration gradient is

$$\left(\frac{dc}{dy}\right)_{y=0} = -\frac{(c_e - c_\infty)_{f_G=0}}{\delta_1} \tag{19}$$

  regardless of any subsequent desorption.
- The gradient of the concentration profile is zero at $f = f_G = 1$ and $y = \delta_1$.

$$\left(\frac{dc}{dy}\right)_{y=\delta_1} = 0 \tag{20}$$

The form

$$\frac{dc}{dy} = -\frac{(c_e - c_\infty)_{f_G=0}}{\delta_1}\left[1 - f_G\left(\frac{y}{\delta_1}\right)^{0.5}\right] \tag{21}$$

meets these conditions. Integration with the boundary condition $c = c_\infty$ at $y = \delta_1$ delivers the concentration profile

$$\frac{c - c_\infty}{(c_e - c_\infty)_{f_G=0}} = 1 - \frac{y}{\delta_1} - \frac{2}{3} f_G\left[1 - \left(\frac{y}{\delta_1}\right)^{1.5}\right] \tag{22}$$

Eq. (22) is shown in Fig. 4. Increasing values of the gas-evolution efficiency f_G increase the curvature of the concentration profile. It is seen that the real concentration $c = c_e$ at the electrode surface,

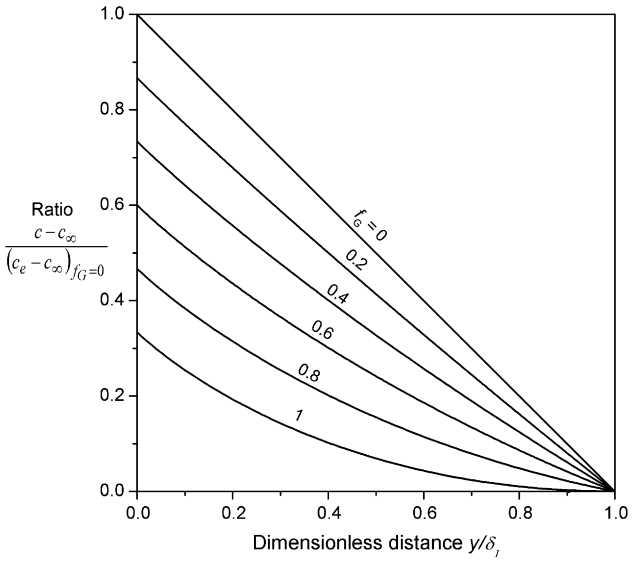

Fig. 4. Concentration profiles, Eq. (22). The curvature depends on the gas-evolution efficiency.

$y = 0$, is lowered as the gas-evolution efficiency increases.

$$\frac{c_e - c_\infty}{(c_e - c_\infty)_{f_G=0}} = 1 - \frac{2}{3} f_G \tag{23}$$

This numerical value coincides with a result previously obtained in a different way [40].

5. Model results

5.1. Model I

Inserting Eqs. (9) and (17) into (12) delivers

$$\frac{df}{dy} = \frac{4}{\bar{d}} \Theta \frac{Sh_2}{Sh_1} \frac{c - c_b}{(c_e - c_\infty)_{f_G=0}} \tag{24}$$

The controlling concentration differences of both processes can be taken into account by

$$\frac{df}{dy} = \frac{4}{\bar{d}} \Theta \frac{Sh_2}{Sh_1} \left[\frac{c - c_\infty}{(c_e - c_\infty)_{f_G=0}} + \frac{c_\infty - c_b}{(c_e - c_\infty)_{f_G=0}} \right] \tag{25}$$

The second term in brackets denotes the relative supersaturation of the liquid bulk. This supersaturation may reach noticeable values [24,32]. However, compared to the electrode boundary layer with (under certain conditions) enormous supersaturation [41–43], the bulk supersaturation is small as pointed out long time ago for hydrogen and oxygen evolution [8]. Freely moving bubbles remaining for some time in the interelectrode gap continue to grow by desorption from the slightly supersaturated liquid. They further lower the supersaturation. So the desorption within the liquid bulk is negligible compared to that in the boundary layer. The supersaturation term will henceforward be disregarded.

$$\frac{c_\infty - c_b}{(c_e - c_\infty)_{f_G=0}} \approx 0 \tag{26}$$

A basic approach will first be made mainly to recognize the quantities relevant for the gas-evolution efficiency. For the sake of simplicity, the curvature of the concentration profile within the boundary layer is ignored and a linear profile is supposed on the basis of Eq. (23).

$$\frac{c - c_\infty}{(c_e - c_\infty)_{f_G=0}} = \left(1 - \frac{2}{3} f_G\right) \left(1 - \frac{y}{\delta_1}\right) \tag{27}$$

The deviation from reality will be the more pronounced the larger the f_G value as seen from Fig. 4. Inserting Eqs. (27) into (25) with (26) gives

$$\frac{df}{dy} = \frac{4}{\bar{d}} \Theta \frac{Sh_2}{Sh_1} \left(1 - \frac{2}{3} f_G\right) \left(1 - \frac{y}{\delta_1}\right) \tag{28}$$

For integration of Eq. (28) two cases must be distinguished. As seen from Eq. (11) nearly spherical bubbles the height $\bar{d}$ of which equals or exceeds the thickness of the diffusion layer are subject to the condition

$$Sh_1 \equiv \frac{d}{\delta_1} \geq 1.5 \tag{29}$$

In this case, desorption takes place within the total electrode boundary layer thickness. Integration of Eq. (28) gives with (16)

$$f_G = 4\Theta \frac{Sh_2}{Sh_1} \left(1 - \frac{2}{3} f_G\right) \int_{y=0}^{\delta_1} \left(1 - \frac{y}{\delta_1}\right) \frac{dy}{\bar{d}} = \left(\frac{1}{3} \frac{Sh_1^2}{\Theta Sh_2} + \frac{2}{3}\right)^{-1} \tag{30}$$

Small bubbles (in relation to the boundary layer thickness),

$$Sh_1 \equiv \frac{d}{\delta_1} \leq 1.5 \tag{31}$$

remain totally within the boundary layer as long as attached to the electrode. The integration limit is now $Y = \bar{d}$.

$$f_G = 4\Theta \frac{Sh_2}{Sh_1} \left(1 - \frac{2}{3} f_G\right) \int_{y=0}^{\bar{d}} \left(1 - \frac{y}{\delta_1}\right) \frac{dy}{\bar{d}}$$

$$= \left(\frac{1/4Sh_1/\Theta Sh_2}{1 - Sh_1/3} + \frac{2}{3}\right)^{-1} \tag{32}$$

Eqs. (30) and (32) coincide for $Sh_1 = 1.5$.

They provide an essential information. It is seen that the gas-evolution efficiency is not only affected by the bubble coverage Θ – as previously stated [44] – but also by the Sherwood numbers Sh_1 and Sh_2 expressing the two competing mass transfer mechanisms. The dimensionless group $(\Theta Sh_2 Sh_1^{-1})$ is the main controlling parameter. Eqs. (30) and (32) are shown in Fig. 5.

5.2. Model II

The above applied model is of such a simplicity that the suspicion may be justified the results could be most doubtful. Therefore, two more models improved in several aspects were established.

When using Eq. (28) in the above approach it was left out of consideration that the concentration gradient dc/dy varies within the boundary layer as preset by Eq. (22). Model I supposes linear concentration profiles. An improvement can be expected when Eq. (22) is inserted into Eq. (25).

$$\frac{df}{dy} = \frac{4}{\bar{d}} \Theta \frac{Sh_2}{Sh_1} \left\{1 - \frac{y}{\delta_1} - \frac{f_G}{1.5} \left[1 - \left(\frac{y}{\delta_1}\right)^{1.5}\right]\right\} \tag{33}$$

Neglecting again the supersaturation of the bulk liquid, integration of Eq. (33) delivers the wanted information about the gas-evolution efficiency. For big bubbles,

$$Sh_1 \equiv \frac{d}{\delta_1} \geq 1.5 \tag{34}$$

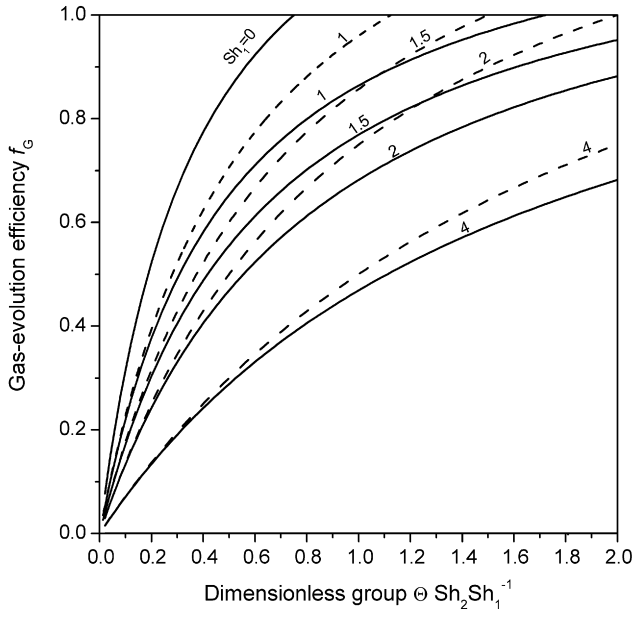

Fig. 5. Visualization of results of models I and II. Broken lines: Eqs. (30) and (32); solid lines: Eqs. (35) and (37).

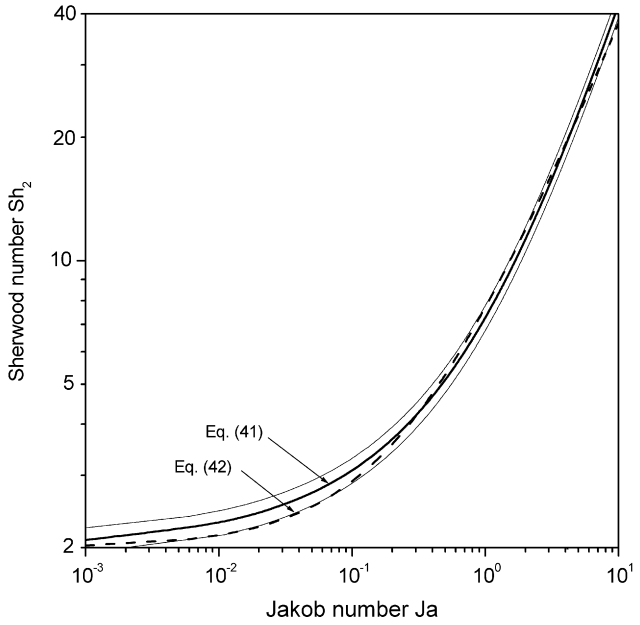

Fig. 6. Comparison of Eq. (41) – solid line – with the approximative Eq. (42) – broken line.

one obtains

$$f_G = 4\Theta\frac{Sh_2}{Sh_1}\int_{y=0}^{\delta_1}\left\{1-\frac{y}{\delta_1}-\frac{f_G}{1.5}\left[1-\left(\frac{y}{\delta_1}\right)^{1.5}\right]\right\}\frac{dy}{\bar{d}}$$

$$= \left(\frac{1}{3}\frac{Sh_1^2}{\Theta Sh_2}+0.8\right)^{-1} \tag{35}$$

and for small bubbles,

$$Sh_1 \equiv \frac{d}{\delta_1} \le 1.5 \tag{36}$$

one obtains

$$f_G = 4\Theta\frac{Sh_2}{Sh_1}\int_{y=0}^{\bar{d}}\left\{1-\frac{y}{\delta_1}-\frac{f_G}{1.5}\left[1-\left(\frac{y}{\delta_1}\right)^{1.5}\right]\right\}\frac{dy}{\bar{d}}$$

$$= \frac{1-Sh_1/3}{1/4Sh_1/\Theta Sh_2+2/3-0.145Sh_1^{1.5}} \tag{37}$$

Eqs. (35) and (37) must again coincide for $Sh_1 = 1.5$. It is recognizable that the dimensionless group $(\Theta Sh_2 Sh_1^{-1})$ plays again a leading role. For big bubbles, the group is simply multiplied by Sh_1 as known from Eq. (30), whereas for small bubbles the impact of Sh_1 is more complex than in Eq. (32).

5.3. Model III

The Sherwood number Sh_1 of mass transfer from the electrode to the liquid bulk, commonly resulting from combined action of microconvective mass transfer, single-phase and two-phase free mass transfer, may be taken from available mass transfer equations [45,1,2].

However, the Sherwood number Sh_2 involves an additional problem. Unlike many other mass transfer mechanisms, the rate of mass transfer in desorption is not only dependent on the concentration difference but also on the Sherwood number which is affected by the concentration difference itself. The dependence is commonly expressed by the Jakob number

$$Ja = \frac{RT}{p}(c-c_b) \tag{38}$$

For small values of the Jakob number, $Ja \to 0$, the Sherwood number for a bubble in an infinite field is constant,

$$Sh_2 = 2 \tag{39}$$

For large values, $Ja \to \infty$, theoretical derivations show a dependence on Ja.

$$Sh_2 = \frac{12}{\pi}Ja \tag{40}$$

A general relationship for a sphere in infinite solution is [38]

$$Sh_2 = 2+\frac{6}{\pi}Ja\left[1+\left(1+\frac{2\pi}{3Ja}\right)^{0.5}\right] = \frac{3}{\pi}Ja\left[1+\left(1+\frac{2\pi}{3Ja}\right)^{0.5}\right]^2 \tag{41}$$

In both the previous models, the Sherwood number Sh_2 has been unrealistically supposed independent of the concentration variation within the boundary layer. In fact, the Jakob number depends on the concentration, as seen from Eq. (38). Consequentially the Sherwood number Sh_2 can no longer be considered constant. For practical handling, Eq. (41) may be approximated by

$$Sh_2 = 2+5.7Ja^{0.8} \tag{42}$$

with a deviation of less than 7% in the range up to $Sh_2 < 10$, which is commonly satisfactory covering a current density range of about 1 A m^{-2} up to 200 000 A m^{-2}, Fig. 6. Inserting Eqs. (14) and (17) into (38) gives

$$Ja = \frac{Pe}{Sh_1}\frac{c-c_b}{(c_e-c_\infty)_{f_G=0}} \tag{43}$$

with the definition of the Péclet number of mass transfer at gas-evolving electrodes

$$Pe \equiv \Phi^*\frac{I/A}{\nu_e/\nu_B F}\frac{RT}{p}\frac{d}{D} \tag{44}$$

Inserting the curved concentration profile, Eq. (22), into Eq. (43) would cause serious problems in integration. Therefore, the curved profile will be restricted to the first concentration term in Eq. (25), whereas a linear profile, Eq. (27), will be used for the Jakob number

$$Ja = \frac{Pe}{Sh_1}\frac{c-c_b}{(c_e-c_\infty)_{f_G=0}} = \frac{Pe}{Sh_1}\left(1-\frac{2}{3}f_G\right)\left(1-\frac{y}{\delta_1}\right) \tag{45}$$

Inserting Eqs. (42) and (45) into (28),

$$f_G = \frac{8\Theta}{Sh_1}\int_0^Y \left\{1 - \frac{y}{\delta_1} - \frac{f_G}{1.5}\left[1 - \left(\frac{y}{\delta_1}\right)^{1.5}\right] + 2.85\left(\frac{Pe}{Sh_1}\right)^{0.8}\left(1 - \frac{2}{3}f_G\right)^{1.8}\left(1 - \frac{y}{\delta_1}\right)^{1.8}\right\}\frac{dy}{\bar{d}} \quad (46)$$

and integration delivers for big bubbles, $d/\delta_1 \equiv Sh_1 \geq 1.5$ and $Y = \delta_1$, an inexplicit expression of the gas-evolution efficiency

$$f_G = \left(\frac{{Sh_1}^2}{6\Theta} + 0.8\right)^{-1}\left[1 + 2.036\left(\frac{Pe}{Sh_1}\right)^{0.8}\left(1 - \frac{2}{3}f_G\right)^{1.8}\right] \quad (47)$$

and for small bubbles, $d/\delta_1 \equiv Sh_1 \leq 1.5$ and $Y = \bar{d}$,

$$f_G = \frac{1 - Sh_1/3 + 1.53(Pe/Sh_1)^{0.8}(1 - 2/3f_G)^{1.8}1/Sh_1[1 - (1 - 2/3Sh_1)^{2.8}]}{Sh_1/8\Theta + 2/3 - 0.145Sh_1^{1.5}} \quad (48)$$

In this case, too, the condition of coincidence of Eqs. (47) and (48) for $Sh_1 = 1.5$ is met.

6. Discussion

6.1. Average concentration and concentration controlling mass transfer

All three models still involve two interesting inadequacies. In the following they will briefly be pointed out showing that they at least partly compensate each other.

A numerical estimate shows that for values of $y/\delta_2 \to 1$ at small values of the concentration c the Sherwood number Sh_2 may become small enough to result in values of the ratio Eqs. (30) and (32) larger than unity. The effect is the more pronounced the larger the bubble coverage Θ. Hence, the estimated values of the gas-evolution efficiency f_G would be too large.

On the other hand, it has been supposed that the concentration c outside the bubble boundary layer does not vary in direction of r, parallel to the electrode, and agrees with the average value on the total cross-sectional area A_a at each position y. That implies a simplification because of the concentration variation within the bubble boundary layer of thickness δ_2.

The inaccuracy may easily be estimated. According to the model assumptions, the concentration gradient within the boundary layer surrounding the adhering bubble is linear. So the concentration c (outside the bubble boundary layer) attains a value corresponding to a cross-sectional area with half the boundary layer thickness. The ratio of the concentration differences is thus

$$\frac{c - c_b}{\bar{c} - c_b} = \frac{A_a}{A_a - A_\delta/2} = \left(1 - \frac{2}{Sh_2^2}\frac{1 + Sh_2}{1/\Theta - 1}\right)^{-1} \quad (49)$$

where A_δ denotes the area occupied by the bubble boundary layer.

The concentration c taken into account is seen to be the more distorted the larger the bubble layer thickness, i.e. the smaller the Sherwood number Sh_2. The effect is the more pronounced the larger the bubble coverage Θ. The obtained gas-evolution efficiency is somewhat too large. The two inefficiencies under discussion act distorting, particularly at small values of Sh_2, but they act antagonistically. They compensate each other at least partly and are not taken into account in all model versions.

6.2. Curvature of the concentration profile

The exponent $m = 0.5$ in Eq. (21) controlling the curvature of the electrode concentration profile seems to be arbitrary. It is not. One can easily make sure that the value must be within the limits $0 < m < 1$. But a further condition must be satisfied. As the electrode tends to be nearly completely blanketed by adhering bubbles, $\Theta \to 1$, the gas-evolution efficiency must approach $f_G \to 1$. Inserting a concentration profile in the general form

$$\frac{c - c_\infty}{(c_e - c_\infty)_{f_G=0}} = 1 - \frac{y}{\delta_1} - \frac{f_G}{1 + m}\left[1 - \left(\frac{y}{\delta_1}\right)^{1+m}\right] \quad (50)$$

into Eq. (25) delivers after integration (with assumption of no supersaturation of the bulk)

$$f_G = \left(\frac{1}{3\Theta}\frac{Sh_1^2}{Sh_2} + \frac{1}{1 + m/2}\right)^{-1} \quad (51)$$

resulting for $f_G \to 1$ and $\Theta \to 1$ in

$$\frac{Sh_1^2}{Sh_2} = \frac{3}{1 + 2/m} \quad (52)$$

Inserting realistic values of the Sherwood numbers for large values of the current density leads to $m = 0.5$ as applied in Eq. (22).

7. Conclusions

The value of the gas-evolution efficiency is indispensable in estimating the mass transfer coefficient in all mechanisms of bubble induced mass transfer. The expected interrelation between bubble coverage Θ and gas-evolution efficiency f_G is confirmed. However, it is by far too easy to simply refer to an available relationship $f_G = f_G(\Theta)$ as proposed in literature [44].

The present analysis evidences quantitatively that the gas-evolution efficiency is the result of the two competing processes of mass transfer to the liquid bulk and to the adhering bubbles. Therefore, f_G is dependent on the Sherwood numbers of each of the processes, Sh_1 and Sh_2, representing the mass transfer coefficients.

The bubble coverage Θ is affected by the rate of formation of product, hence on the nominal current density, and further on the mean bubble diameter in addition to the wettability acting on the number of simultaneously adhering bubbles.

f_G mainly depends on a relevant dimensionless group $(\Theta Sh_2 Sh_1^{-1})$. Additionally, under certain conditions, the Sherwood number Sh_1 of mass transfer to the liquid bulk appears separately, e.g. in Eqs. (30) and (32).

The diffusion coefficient of dissolved gas in liquid is equally of impact on mass transfer to liquid bulk as well as to adhering bubbles. So it does not appear in the dimensionless group $(\Theta Sh_2 Sh_1^{-1})$. Nonetheless, it is active wherever the Sherwood number Sh_1 appears separately.

At incomplete desorption, $f_G < 1$, the to liquid bulk is supersaturated. Owing to the presence of freely moving bubbles in the interelectrode gap the supersaturation is moderate, but noticeable. In case of big bubbles, i.e. large values of the current density, the supersaturation of the bulk may additionally act on the gas-evolution efficiency. This impact might be small and has not been taken into account.

The gas-evolution efficiency f_G denotes the fraction of the total dissolved gas that is absorbed by bubbles adhering to the electrode surface. This value is the controlling one in estimating the rate of the microconvective mass transfer. The total amount of absorbed gas in an electrochemical reactor is larger than given by the present equations in all cases where the desorption by adhering bubbles is incomplete and continues in the liquid bulk to freely moving bubbles. Therefore, values of the gas-evolution efficiency obtained experimentally by collecting the evolved gas [46] are larger than the quantity in the present definition.

A numerical analysis of the present results will be published separately in part II.

References

[1] H. Vogt, Electrochim. Acta 38 (1993) 1421.
[2] H. Vogt, Electrochim. Acta 38 (1993) 1427.
[3] L.J.J. Janssen, E. Barendrecht, Electrochim. Acta 24 (1979) 693.
[4] G.M. Whitney, C.W. Tobias, AIChE J. 34 (1988) 1981.
[5] G. Bendrich, W. Seiler, H. Vogt, Int. J. Heat Mass Transfer 29 (1986) 1741.
[6] H. Vogt, Electrochim. Acta 32 (1987) 633.
[7] J. Eigeldinger, H. Vogt, Electrochim. Acta 45 (2000) 4449.
[8] H. Vogt, Electrochim. Acta 25 (1980) 527.
[9] R. Wedin, L. Davoust, A. Cartellier, P. Byrne, Exp. Thermal Fluid Sci. 27 (2003) 685.
[10] H. Vogt, R.J. Balzer, Electrochim. Acta 50 (2005) 2073.
[11] H. Vogt, Electrochim. Acta 29 (1984) 167.
[12] H. Vogt, Electrochim. Acta 29 (1984) 175.
[13] E. Baars, C. Kayser, Z. Elektrochem. 36 (1930) 428.
[14] A. Eucken, Lehrbuch der chemischen Physik, 2. Aufl., Bd. 2, Akad. Verlagsges, Leipzig, 1944.
[15] I. Roušar, V. Cezner, Electrochim. Acta 20 (1975) 289.
[16] I.V. Kadija, V.M. Nakić, J. Electroanal. Chem. Interf. Chem. 34 (1972) 15.
[17] I.V. Kadija, V.M. Nakić, J. Electroanal. Chem. Interf. Chem. 35 (1972) 177.
[18] I.V. Kadija, B.Ž. Nikolić, A.R. Despić, J. Electroanal. Chem. Interf. Chem. 57 (1974) 35.
[19] H. Vogt, Chemie-Ing. -Technik 52 (1980) 418.
[20] H. Vogt, Electrochim. Acta 26 (1981) 1311.
[21] C.W.M.P. Sillen, Dissertation Tech. Hogeschool Eindhoven, 1983.
[22] L.J.J. Janssen, C.W.M.P. Sillen, E. Barendrecht, S.J.D. van Stralen, Electrochim. Acta 29 (1984) 633.
[23] L. Müller, M. Krenz, L. Landsberg, J. Electroanal. Chem. 180 (1984) 453.
[24] H. Vogt, Electrochim. Acta 30 (1985) 265.
[25] L.J.J. Janssen, E. Barendrecht, Electrochim. Acta 30 (1985) 683.
[26] N.P. Brandon, G.H. Kelsall, J. Appl. Electrochem. 15 (1985) 475.
[27] J.M. Chin Kwie Joe, L.J.J. Janssen, S.J.D. van Stralen, J.H.G. Verbunt, W.M. Sluyter, Electrochim. Acta 33 (1988) 769.
[28] C. Gabrielli, F. Huet, M. Keddam, A. Macias, A. Sahar, J. Appl. Electrochem. 19 (1989) 617.
[29] J. St-Pierre, N. Massé, M. Bergeron, Electrochim. Acta 40 (1995) 1013.
[30] D.T. Shieh, B.J. Hwang, J. Electroanal. Chem. 391 (1995) 77.
[31] H. Matsushima, D. Kiuchi, Y. Fukunaka, K. Kuribayashi, Electrochem. Commun. 11 (2009) 1721.
[32] B. Krause, H. Vogt, J. Appl. Electrochem. 15 (1985) 509.
[33] P.J. Sides, C.W. Tobias, J. Electrochem. Soc. 127 (1980) 288.
[34] M. Krenz, L. Müller, A. Pomp, Electrochim. Acta 31 (1986) 723.
[35] J. Dukovic, C.W. Tobias, J. Electrochem. Soc. 134 (1987) 331.
[36] H. Vogt, Z. Phys. Chem. 172 (1991) 123.
[37] W.M. Buehl, J.W. Westwater, Am. Inst. Chem. Engrs. J. 12 (1966) 571.
[38] H.F.A. Verhaart, R.M. de Jonge, S.J.D. van Stralen, Int. J. Heat Mass Transfer 23 (1980) 293.
[39] H. Riegel, J. Mitrovic, K. Stephan, J. Appl. Electrochem. 28 (1998) 10.
[40] H. Vogt, J. Appl. Electrochem. 19 (1989) 713.
[41] S. Shibata, Bull. Chem. Soc. Jpn. 36 (1963) 53.
[42] V.G. Nefedov, V.M. Serebritskii, V.V. Matveev, O.S. Ksenzhek, Elektrokhim 27 (1991) 1625;
V.G. Nefedov, V.M. Serebritskii, V.V. Matveev, O.S. Ksenzhek, Sov. Elektrochem. 27 (1991) 1427.
[43] H. Vogt, J. Appl. Electrochem. 23 (1993) 1323.
[44] H. Vogt, J. Electrochem. Soc. 137 (1990) 1179.
[45] K. Stephan, H. Vogt, Electrochim. Acta 24 (1979) 11.
[46] L. Müller, M. Krenz, K. Rübner, Electrochim. Acta 34 (1989) 305.